



Synthesis and characterization of Dawson heteropolyanion $[H_3Fe][\alpha_2P_2MoW_{17}O_{62}]$: application on dye degradation

Nawel Nadji^{a,b}, Robila Belghiche^{c,*}, Denis Merlet^d

^aLaboratory of Environmental Engineering, Faculty of Engineering, Department of Process Engineering, Badji Mokhtar-Annaba University, P.O.Box 12, 23000 Annaba, Algeria, Tel. +213 675668266; email: nadji_n@yahoo.fr

^bResearch Centre in Analytical Chemistry and Physics, (CRAPC), BP 384, Siège ex-Pasna Zone Industrielle, Bou-Ismaïl, 42004 Tipaza, Algeria, Tel. +213 675668266; email: nadji_n@yahoo.fr

^cLaboratory of Chemistry Inorganic Materials, Faculty of Science, Department of Chemistry, Badji Mokhtar-Annaba University, P.O.Box 12, 23000 Annaba, Algeria, Tel. +213 663320321; email: robuniv@yahoo.fr

^dLaboratory NMR Oriented Environment, Paris-Sud 11 University, Bâtiment 420, 91405 Orsay, France, Tel. +33 169157432; email: denis.merlet@u-psud.fr

Homage to Prof. Mostefa Abbessi, Professor in Process Engineering Department, Faculty of Engineering Sciences, who passed away on December 31, 2015

Received 2 February 2016; Accepted 27 July 2016

ABSTRACT

An heteropolyanion compound consisting of saturated Dawson anions and trivalent iron cations, $\alpha_2H_3FeP_2W_{17}MoO_{62}$ has been synthesized and characterized by various spectroscopic methods, IR, UV-Vis, ³¹P NMR and ESI-MS. The catalytic performances of heteropolyanion were tested for degradation of aqueous Malachite Green dye under Fenton process. The degradation reaction was monitored by UV-visible and IR spectroscopy. The effects of different reaction parameters such as the initial pH of the medium, the initial hydrogen peroxide concentration, the catalyst mass, the initial MG concentration and the reaction temperature on the oxidative degradation of malachite green has been investigated. The optimal reacting conditions were found to be pH = 3, initial hydrogen peroxide was 0.31 M, and the catalyst mass was 0.03 g, for initial MG concentration of 20 mg.L⁻¹ at 30°C. After optimizing operating parameters, the dye was demineralized after 7 h of reaction.

Keywords: Heteropolyanion; Synthesis; Characterization; Catalysis; dye; Degradation; Wastewater treatment

1. Introduction

Environmental pollutants, such as synthetic dyes, have been a threat to our society. These substances are recalcitrant molecules, toxic to microorganisms and are liable to affect the hormonal system without inducing direct toxicological risks on human beings and wildlife. Due to their good solubility, synthetic dyes are common water pollutants and are frequently found in industrial wastewater [1,2]. Particularly triphenylmethane dyes, Malachite green (MG), or C.I. Basic

green 4, is a cationic dye used in different domains. Malachite green has been extensively used in textile industry for dyeing wool and silk, paper, and in leather industry [3–7]. Besides its industrial uses, has widely been used to prevent fungal infections in fish farms [8]. If discharged malachite green directly into streams, it will affect the aquatic lives and cause detrimental effects on the liver, gill, kidney, intestine, gonads and pituitary gonadotropic cell of casualty.

Advanced oxidation processes are an alternative promising compared to the traditional treatment processes of effluent. Removal of colour and recalcitrant organic content of textile effluent can be achieved with the high efficiencies. Costs

* Corresponding author.

of AOPs are another point of view. But, Fenton process seems to be viable choice for textile wastewater treatment [9,10]. Fenton reaction has attracted attention because of its simplicity, rapidity and highly efficiency in organic contaminant removal. If the concentrations of reactants are not limiting, the organic compounds can be completely mineralized. The classical Fenton reaction is based on the activation of hydrogen peroxide (H_2O_2) by aqueous ferrous iron (Fe(II)) under acidic conditions to form hydroxyl radicals, $\cdot OH$. Several studies have reported that other cations such as Fe^{3+} , Cu^{2+} , Mn^{2+} , Co^{2+} can also mediate the Fenton reaction, these reactions are referred to as the “Fenton-like processes” [11,12].

Heteropolyanions (HPAs) are metal-oxo clusters, are stable and easily modified by incorporation of transition metal ions. This family of clusters has been widely applied in various fields, including catalysis [13–15] and electrocatalysis [16,17]. The heteropolyanions obtained with P constitute a rich family. Two main types of heteropolyanions are known, the type of Keggin [$PW_{12}O_{40}$] $^{3-}$ and type of Dawson [$P_2W_{18}O_{62}$] $^{6-}$ (Fig. 1).

The ability to modify the redox and chemical properties of heteropolyanions by replacing and or introducing one or more elements renders them particularly interesting in catalysis.

In this work we report the synthesis, characterization and catalytic properties of a new heteropolyanion complex formed by introducing Fe (III) ion into the saturated 17-tungsto-1-molybdo-2-phosphate mixed heteropolyanion [$P_2MoW_{17}O_{62}$] $^{6-}$.

The addition of ferric ions at the acid form was made by analogy to the compounds $[(M(H_2O)_4)_x][H_{6-2x}P_2W_{18-n}MoO_{62}]$ ($M = Cu^{II}, Co^{II}, Ni^{II}$) [18] and leads to the compound [$H_3FeP_2MoW_{17}O_{62}$], which is characterized by IR, UV, ^{31}P NMR.

The catalytic oxidation of malachite green in aqueous solution, in the presence of Dawson heteropolyanion [$H_3P_2W_{18}O_{62}$], has been studied by photocatalytic process [19]. In this work, we have investigated the oxidation of malachite

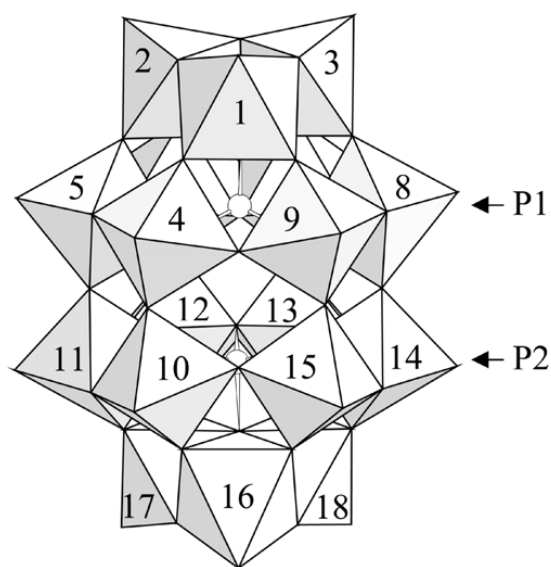


Fig. 1. Structure of Dawson.

green by [$H_3FeP_2MoW_{17}O_{62}$] Dawson heteropolyanion with Fenton catalytic process as well as the influence of operating parameters on the decolorization such as oxidant dosages; initial dye concentration, pH of solution, catalyst mass and temperature were determined to find optimum conditions for complete decolorization and total oxidation of dye solution.

2. Materials and methods

2.1. Synthesis of precursor heteropolyanions

The heteropolyanions $K_6P_2W_{18}O_{62}$, $\alpha_2K_{10}P_2W_{17}O_{61}$ and $\alpha_2K_6P_2W_{17}MoO_{62}$ were synthesized according to the published procedures [20,21]. The structure and purity of $\alpha_2K_6P_2W_{17}MoO_{62}$ were confirmed by infrared, ^{31}P NMR and ESI mass spectroscopy. The acid form of mixed salt $\alpha_2K_6P_2W_{17}MoO_{62}$ was prepared by extraction with ether.

2.2. Synthesis of $H_3FeP_2W_{17}MoO_{62}$ (HPAFe)

A 0.178 g (1.1 mmole) of $FeCl_3$ was dissolved in 20 mL of water at room temperature after stirring, 5 g (1.1 mmole) of $H_6P_2W_{17}MoO_{62} \cdot 14H_2O$ was then added. The mixture was stirred for 10 min. Dark yellow crystals were obtained after 4 d by slow evaporation with yield 76%. UV-Visible: shoulder between 198 and 282 nm for $[HPAFe] = 6.82 \times 10^{-5}$ M.

2.3. Characterization of heteropolyanions

BET surface area measurement was performed at liquid nitrogen temperature using a Micrometrics ASAP 2020 apparatus. The sample was degassed at $T = 80^\circ C$ for 4 h.

The IR spectra were recorded on KBr pellets using a spectrophotometer shimadzu FTIR-8400s. The UV-visible spectra were recorded on spectrophotometer Jenway 6300 UV/visible in a quartz cell. ^{31}P NMR spectra were recorded on Bruker 400 MHz Ascend. The ^{31}P NMR shifts were measured for 10^{-3} M solution of heteropolyanions in D_2O solution and were referenced to 85% H_3PO_4 . The ESI mass spectra were recorded in negative mode on microtof-Q II 10027 Bruker electro spray ionization mass spectrometer. The capillary high voltage was set to +3,000 V. The end voltage was set to -500 V.

2.4. Oxidation of malachite green (MG) dye

The dye, malachite green oxalate salt of chemical formula $C_{25}H_{36}N_4O_{12}$, was purchased from Sigma-Aldrich without any purification. The structure of this dye is shown in Fig. 2 [22].

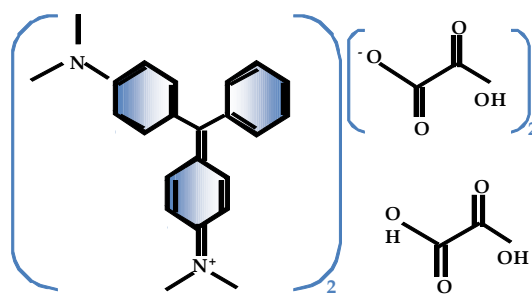


Fig. 2. Chemical structure of malachite green.

The oxidation of the dye with hydrogen peroxide (H_2O_2 , 30%) in the presence of heteropolyanion was performed as follows: A given quantity of heteropolyanion was added to 100 mL of malachite green solution (5 mg/L). After vigorous stirring in a thermostatic bath (25°C), the pH of the solution is adjusted with H_2SO_4 (0.1N) or NaOH (0.1N) before addition of the oxidant H_2O_2 . The concentrations of malachite green in solution were analysed with different time intervals.

The malachite green concentrations were analysed at the maximum wavelength ($\lambda_{\text{max}} = 619 \text{ nm}$) with UV-Vis spectrophotometer. Hydrogen peroxide concentrations were determined using the iodometric method.

The degradation efficiency of malachite green was defined as follows:

$$E (\%) = [(C_i - C_f) / C_i] \times 100$$

where C_i (mg/L) is the initial concentration of malachite green, and C_f (mg/L) is the final dye concentration at reaction time t (min).

3. Results and discussion

3.1. Synthesis and characterization

The heteropolyanion $\alpha_2\text{K}_6\text{P}_2\text{W}_{17}\text{MoO}_{62} \cdot n\text{H}_2\text{O}$ and the corresponding acid form were prepared as described in the literature [23]. $\alpha_2\text{K}_6\text{P}_2\text{W}_{17}\text{MoO}_{62}$ heteropolyanion is saturated mixed specie derived from the Dawson structure; it was obtained by substitution of an apical tungsten with a molybdenum. The corresponding acid form is obtained by extraction with ether under acidic conditions. The addition of ferric ions at the acidic form of saturated 17-tungsto-1-molybdo-2-phosphate mixed heteropolyanion $[\text{P}_2\text{MoW}_{17}\text{O}_{62}]^{6-}$ with 1/1 stoichiometric amounts led to the substitution of three protons. The compound obtained $\alpha_2\text{H}_3\text{FeP}_2\text{W}_{17}\text{MoO}_{62} \cdot n\text{H}_2\text{O}$ was characterized with various spectroscopic methods.

The specific surface area of compound is $4.7105 \text{ m}^2/\text{g}$. The UV-Vis spectrum (Fig. 3) was recorded in aqueous solutions. The W (VI) and Mo(VI) ions have a d^0 electronic

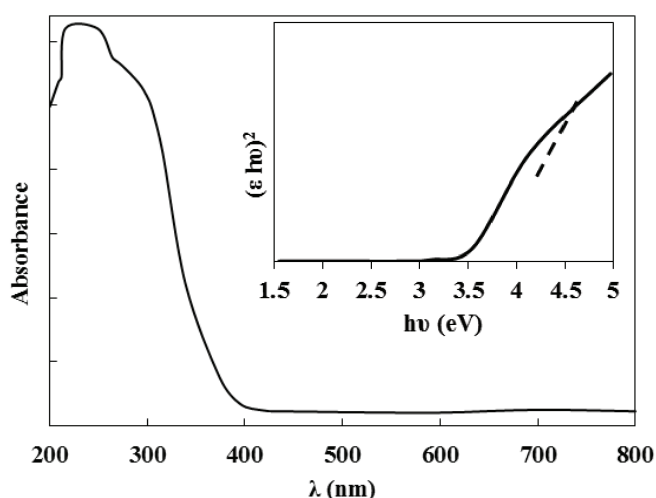


Fig. 3. U.V. spectrum of $[\text{H}_3\text{Fe}][\alpha_2\text{P}_2\text{MoW}_{17}\text{O}_{62}]$.

configuration. The spectrum of the compound show a band between 200 and 280 nm assigned to the π - d electronic transition in M-O terminal [24]. The wide band observed at 300 nm is assigned to electronic transitions in binding M-Ob-M (M = W, Mo) [24]. Gap energy E_g was determined from the UV-visible spectrum [25]. Plot of $(\epsilon hu)^2$ against hu is shown in inset of Fig. 3. The extrapolated value of hn at $\epsilon = 0$ (ϵ is the absorption coefficient) gave an absorption edge energy at $E_g = 3.5 \text{ eV}$.

The IR spectra of synthesized heteropolyanions have all characteristic bands of Dawson structure (Table 1) [26,27]. The IR spectrum of compound $\alpha_2\text{H}_3\text{FeP}_2\text{W}_{17}\text{MoO}_{62}$ shows a band at $1,092 \text{ cm}^{-1}$ attributed to the asymmetric vibration of the P-Oa bond. The bands located at 960 , 914 and 783 cm^{-1} assigned, respectively to asymmetric vibrations of M-O terminal groups and inter- and intra-M-O-M (M = W, Mo).

The phosphorus NMR spectroscopy is particularly suitable for checking the purity of heteropolyanions. ^{31}P NMR spectrum of $\alpha_2\text{K}_6\text{P}_2\text{W}_{17}\text{MoO}_{62}$ shows two peaks located at -12.23 and -13 ppm (Fig. 4(a)), indicating the two in equivalence phosphorus in this structure. These values are comparable to those observed by [20]. $\alpha_2\text{H}_3\text{FeP}_2\text{W}_{17}\text{MoO}_{62}$ is a product with a single peak on the ^{31}P NMR spectrum located -13.208 ppm (Fig. 4(b)). The second phosphorus resonance, near the ferric ion affected by its paramagnetism is radically shifted and broadened. This shift and broadening is enough important to make the corresponding signal unobserved [28,29].

The ESI mass spectrum of $\alpha_2\text{H}_3\text{FeP}_2\text{W}_{17}\text{MoO}_{62}$ (Fig. 5) displays a base peak centered at $m/z = 1,064.71$ and another peak at $m/z = 1,419.26$. These peaks characterized by $\Delta(m/z) = 1/4$ and $\Delta(m/z) = 1/3$ were attributed to $(\text{H}_2\text{P}_2\text{W}_{17}\text{MoO}_{62})^-$ and $(\text{H}_3\text{P}_2\text{W}_{17}\text{MoO}_{62})^{-3}$, respectively.

3.2. Oxidation of malachite green (MG)

3.2.1. Effect of operating conditions on the degradation of malachite green

Several operating conditions affected the degradation of malachite green with H_2O_2 /HPA system such as pH, concentration of malachite green, catalyst mass, reaction temperature and hydrogen peroxide concentration were investigated.

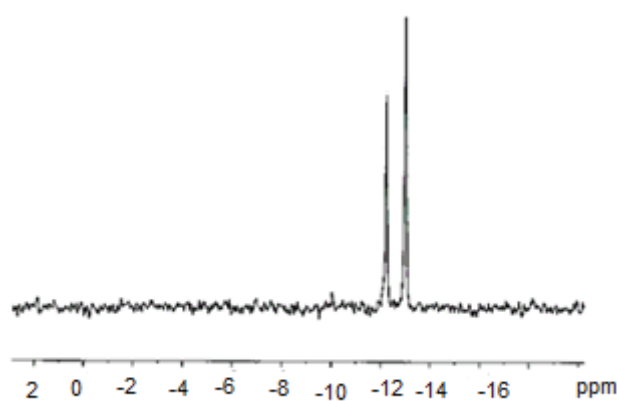
3.2.1.1. Effect of initial pH

The solution pH is one of the most important factors that control the degradation of malachite green. The effect of initial pH on the degradation of malachite green by hydrogen peroxide using $\alpha_2\text{H}_3\text{FeP}_2\text{W}_{17}\text{MoO}_{62}$ as catalyst was determined at the initial dye solution of 5 mg/L, catalyst mass 0.01 g, initial hydrogen peroxide concentration of 0.08 M, and temperature of 25°C. Degradation experiments were performed at different pH values of 2.0, 3.0, 4.0, 6.0, 8.0 and 10.0 to evaluate the MG degradation efficiency of the catalytic oxidation process.

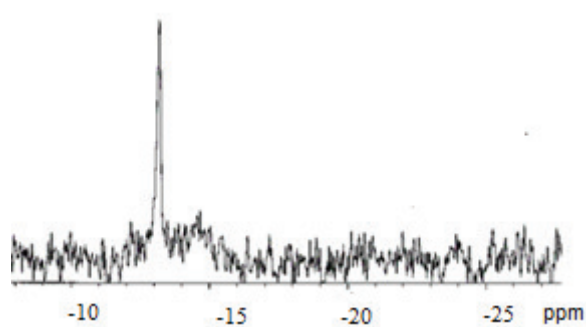
The effect of initial pH on the removal rate of the dissolved dye in the batch Fenton is shown in Fig. 6. The oxidation reaction of malachite green is quite important in acidic media (pH 2, 3, 4, 6) and particularly, faster at pH 3 with maximum degradation efficiency (78.48%) after 120 min.

Table 1
I.R. bands of heteropolyanions

Compound	I.R. bands (cm ⁻¹) $\nu_{as}(P-O_a)$	$\nu_{as}(W-O_d)$	$\nu_{as}(W-O_b-W)$	$\nu_{as}(W-O_c-W)$
$\alpha_2P_2W_{17}O_{61}$	1,086	959	914, 893	800
$\alpha_2P_2W_{17}MoO_{62}$	1,088	960	914	775
$\alpha_2H_3FeP_2W_{17}MoO_{62}$	1,092	960	914	783



(a)



(b)

Fig. 4. ³¹P NMR spectrum of heteropolyanions: $\alpha_2K_6P_2W_{17}MoO_{62}$ (a), $\alpha_2H_3FeP_2W_{17}MoO_{62}$ (b).

Further increase in the pH value from 6 to 10, the degradation efficiency decrease from 68.22% to 48.06%. This was due to that the number of hydroxyl radicals available for degradation of dye reduced when the pH value was greater than six, because, H₂O₂ was unstable in high alkaline solution, and partly decomposed to H₂O and O₂ [30]. Thus, the catalytic activity of HPA was apparently decreased when the solution pH was 10. The rate of degradation of the dye depends on the pH of the medium and the best pH for this reaction was obtained at 3.

3.2.1.2. Effect of $\alpha_2H_3FeP_2W_{17}MoO_{62}$ mass

Catalyst mass can have a significant impact on the dye degradation. To evaluate the influence of $\alpha_2H_3FeP_2W_{17}MoO_{62}$ mass on the degradation, a set of experiments were carried

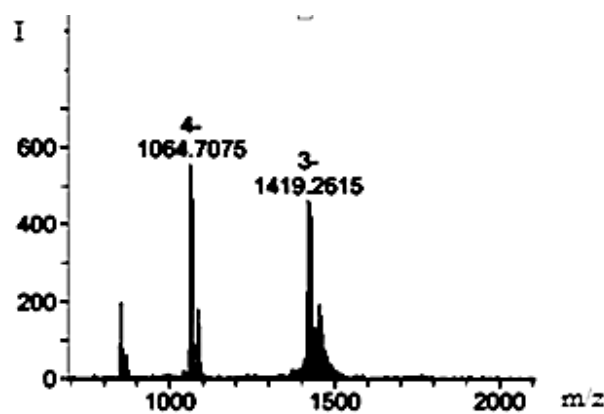


Fig. 5. ESI Mass spectrum of $\alpha_2H_3FeP_2W_{17}MoO_{62}$.

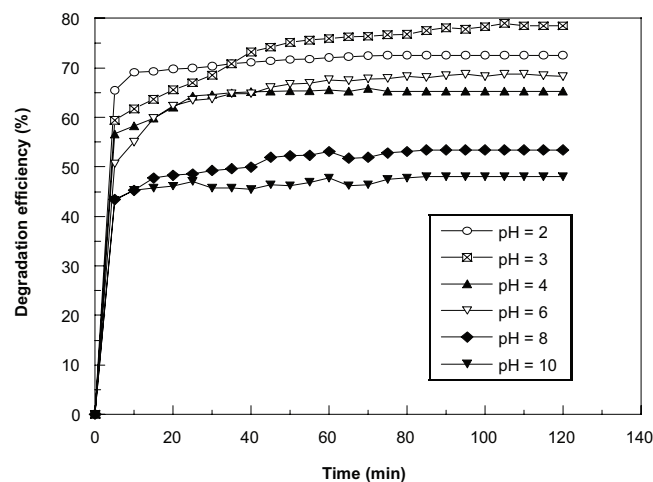


Fig. 6. Effect of initial pH on the degradation of malachite green during Fenton oxidation catalysed by $\alpha_2H_3FeP_2W_{17}MoO_{62}$ (Conditions: $V_R=100$ mL, $[MG]_0=5$ mg/L, $m_{cat}=0.01$ g, $T=25^\circ C$, $[H_2O_2]=0.08$ M).

out by varying the mass from 0 to 0.08 g at optimal pH value (pH = 3), the results are presented in Fig. 7.

The reaction of degradation without catalyst ($m = 0$ g) was produced with a low efficiency (13.70%) after 90 min, but a notable increase of efficiency (13.70% to 67.08%) was observed when the catalyst mass was increased from 0 to 0.005 g. The presence of $\alpha_2H_3FeP_2W_{17}MoO_{62}$ as catalyst significantly increased the degradation rate of malachite green. The presence of catalyst iron-substituted may increase oxidation activity by hydrogen peroxide which favors the formation of hydroxyl radical. The efficiency of degradation is substantially

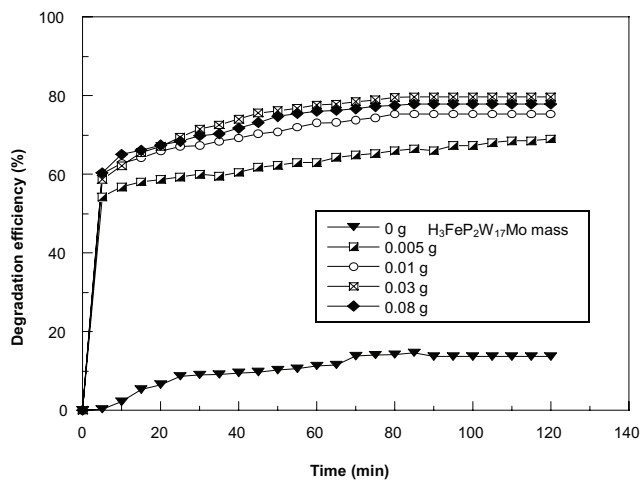


Fig. 7. Effect of catalyst mass on the degradation of malachite green during Fenton oxidation catalysed by $\alpha_2\text{H}_3\text{FeP}_2\text{W}_{17}\text{MoO}_{62}$ (Conditions: $V_R = 100$ mL, $[\text{MG}]_0 = 5$ mg/L; $\text{pH} = 3$, $T = 25^\circ\text{C}$, $[\text{H}_2\text{O}_2] = 0.08$ M).

similar from 0.01 to 0.03 g. However, the degradation efficiency increased less when catalyst mass addition was higher than 0.03 g. The highest efficiency ($E = 79.80\%$) of dye degradation was observed for 0.03 g catalyst mass after 90 min.

3.2.1.3. Effect of initial concentration of hydrogen peroxide

The concentration of H_2O_2 is an important factor in the oxidation reaction by Fenton process. The effect of initial concentration of hydrogen peroxide on malachite green degradation was investigated at optimal parameters of pH and catalyst mass in the range of 0.032 to 0.40 M and the results are shown in Fig. 8.

As expected, the increase in initial $[\text{H}_2\text{O}_2]$ accelerated the dye decolorization at the beginning of the reaction. The decoloration efficiency increased from 63.99% to 81.21% as a consequence of increasing H_2O_2 dosage from 0.032 to 0.31 M. This can be explained by the effect of $\cdot\text{OH}$ radicals produced additionally. The addition of H_2O_2 is known to increase the rate of dye degradation by allowing an enhancement in the yield of formation of hydroxyl radical. On increasing concentration of hydrogen peroxide from 0.31 to 0.40 M, there is no significant variation in the color removal and the degradation efficiency was not significantly changed (81.21%–82.44%). This observation can be explained by deficiency of $\cdot\text{OH}$ radicals in the reaction medium. Similar observations have been reported in other studies [31,32], the H_2O_2 became an extractor of hydroxyl radicals at high concentrations. Thus, increasing concentration of H_2O_2 does not increase the degradation efficiency. For this purpose, an intermediate concentration of 0.31 M in H_2O_2 is chosen for optimum concentration because more H_2O_2 cannot improve the degradation rate much more.

3.2.1.4. Effect of temperature

The increase in temperature accelerated the dye degradation at the beginning of the reaction (Fig. 9). It was observed that the degradation efficiency of malachite green increased

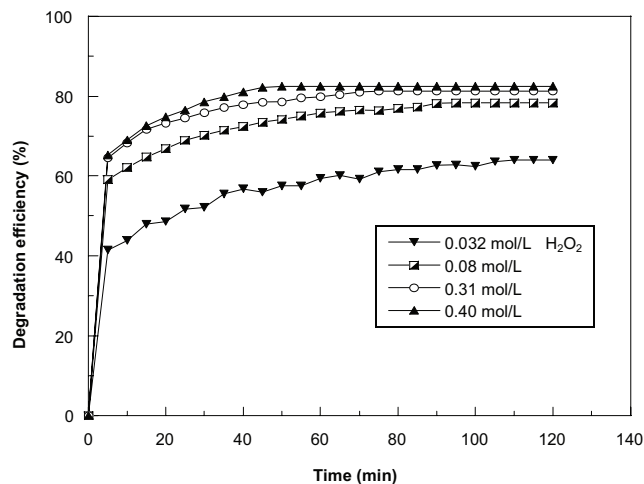


Fig. 8. Effect of initial H_2O_2 concentration on the degradation of malachite green during Fenton oxidation catalysed by $\alpha_2\text{H}_3\text{FeP}_2\text{W}_{17}\text{MoO}_{62}$ (Conditions: $V_R = 100$ mL, $[\text{MG}]_0 = 5$ mg/L; $\text{pH} = 3$, $m_{\text{cat}} = 0.03$ g, $T = 25^\circ\text{C}$).

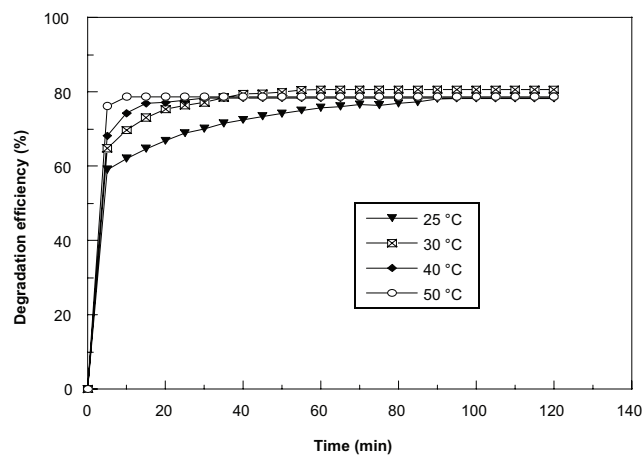


Fig. 9. Effect of temperature on the degradation of malachite green during Fenton oxidation catalysed by $\alpha_2\text{H}_3\text{FeP}_2\text{W}_{17}\text{MoO}_{62}$ (Conditions: $V_R = 100$ mL, $[\text{MG}]_0 = 5$ mg/L; $\text{pH} = 3$, $m_{\text{cat}} = 0.03$ g, $[\text{H}_2\text{O}_2] = 0.31$ M).

from 70.17% to 78.71% as a consequence of increasing the temperature from 30°C to 50°C within the first 30 min of oxidation process. This is because higher temperature increased the reaction rate between hydrogen peroxide and catalyst, thus increasing the rate of generation of oxidizing species such as OH radicals [22]. After a reaction time of 50 min, the increase in the degradation efficiencies of MG (79.97, 78.34 and 78.71) is only marginal on increasing the temperature (30, 40 and 50). Therefore, the temperature 30°C is selected for further study.

3.2.1.5. Effect of initial malachite green concentration

The effect of initial malachite green concentration on the oxidation reaction at the optimized operating parameters (pH, catalyst mass, $[\text{H}_2\text{O}_2]$ and temperature) was studied by varying its concentration in the range of 3–50 mg/L (Fig. 10).

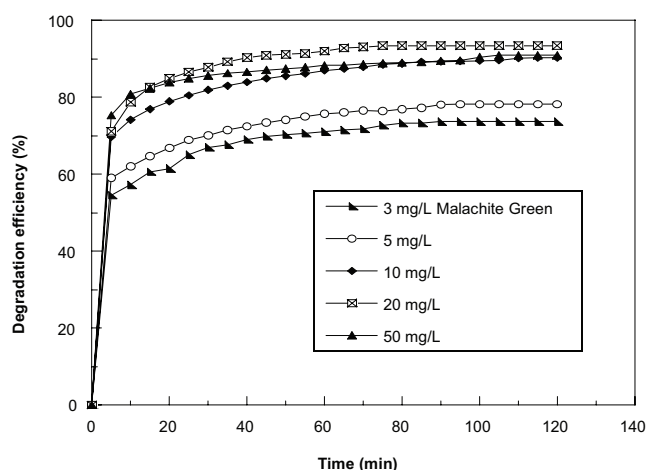


Fig. 10. Effect of initial dye concentration on the degradation of malachite green during Fenton oxidation catalysed by $\alpha_2\text{H}_3\text{FeP}_2\text{W}_{17}\text{MoO}_{62}$ (Conditions: $V_R = 100$ mL, $\text{pH} = 3$, $m_{\text{cat}} = 0.03$ g, $[\text{H}_2\text{O}_2] = 0.31\text{M}$, $T = 30^\circ\text{C}$).

The efficiency of catalytic degradation increased with increasing initial concentration of malachite green from 3 to 20 mg/L (73.66%–93.45%) after 120 min. This phenomenon was due to the effectiveness of hydroxyl radicals produced by the used catalytic system. But a notable decrease (93.45%–90.99%) could be found when the initial concentration was increased from 20 to 50 mg/L. This is probably due to the weakness of available hydrogen peroxide quantities and the degradation of malachite green slowed down significantly. Therefore, the best initial malachite green concentration 20 mg/L.

3.3. Products of malachite green identified by UV-Visible and IR analysis

3.3.1. UV-Visible analysis

UV-Visible spectral analysis of malachite green before degradation and after 80 min of decolorization reaction is presented in Fig. 11. The spectrum showed the disappearance of bands located at 629 and 425 nm relative to the electronic transitions in the $\text{C}=\text{C}$ and $\text{C}=\text{N}$ bonds, respectively [32]. Therefore, the conjugated system has been interrupted by breakdown of $\text{C}=\text{C}$ and $\text{C}=\text{N}$ bonds. TLC check, with different eluent (CHCl_3 , CH_2Cl_2) confirmed the occurrence of two species of significantly different polarities.

The spectrum presented in Fig. 11, also showed the appearance of three bands between 300 and 200 nm. This interval is specific to electronic transitions $\pi-\pi^*$ and $n-\pi^*$ in unsaturated molecules and the carbonyl derivatives [33].

3.3.2. IR analysis

To identify species produced by the degradation of the malachite green, an IR spectrum was performed (Fig. 12) in the dichloromethane. The spectrum of malachite green after 120 min of oxidation revealed the appearance of two bands at 1,010 and 1,090 cm^{-1} which can be attributed to the vibrations of $\text{C}-\text{O}$ bonds of the alcohol function [34] and a band

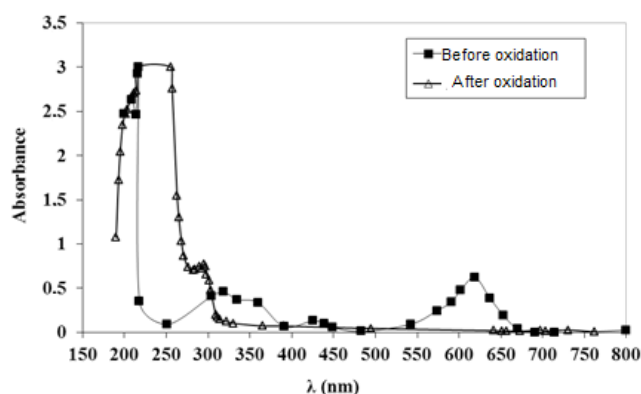


Fig. 11. U.V. spectra of Malachite green before and after 2 h of MG oxidation.

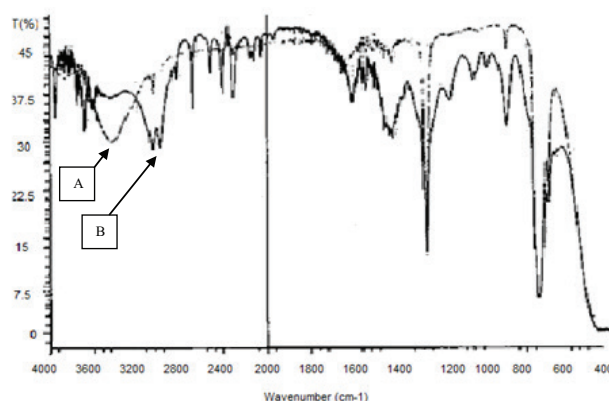


Fig. 12. I.R. spectrum of malachite green before (A) and after 2 h (B) of MG oxidation.

at 1,200 cm^{-1} is attributed to stretching vibration of the $\text{C}-\text{N}$ bond. Two bands located at 1,419 and 1,650 cm^{-1} are related to the $\text{N}-\text{Ph}$ and $\text{C}=\text{O}$ bonds, respectively [34]. Several bands appeared in the range of 2,000–2,900 cm^{-1} are attributed to vibrations of aromatic $\text{C}-\text{H}$ bonds in the benzophenone [34]. The bands located at 3,500 and 3,690 cm^{-1} are related to the vibrations of OH alcohols bonds.

From spectroscopic UV-visible and IR data, Fig. 13 show the products obtained after 2 h of green malachite oxidation.

The IR spectrum of the MG after 4 h of oxidation was very different from that recorded at 2 h of reaction, which revealed the progress of the oxidation reaction.

The IR spectrum of the malachite green after 4 h of oxidation presented bands located at 865.98, 894.91 and 938.27 cm^{-1} relating to the vibration of angular deformation of the $\text{C}-\text{H}$ bonds of the aromatic rings and the stretching vibrations are present at 3,055.03 cm^{-1} . The bands observed at 1,014.49 and 1,097.49 cm^{-1} are attributed to $\text{C}-\text{O}$ bonds of carboxylic acids. Two bands located at 1,369.37 and 1,398.30 cm^{-1} are related to the vibration of $\text{N}-\text{C}$ bonds of CH_3-N fragment. The band at 1,411.80 cm^{-1} corresponds to the vibration of the $\text{N}-\text{Ph}$ bond.

The $\text{C}=\text{O}$ group of the carboxylic acid was present in these bands located at 1,751.24 and 1,757.03 cm^{-1} . The bands

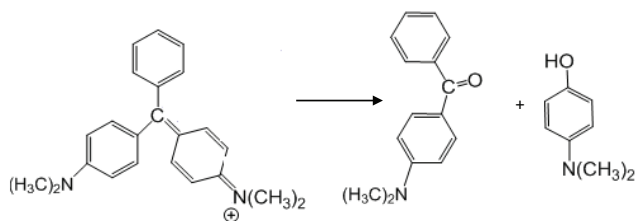


Fig. 13. Products of 2 h of MG oxidation.

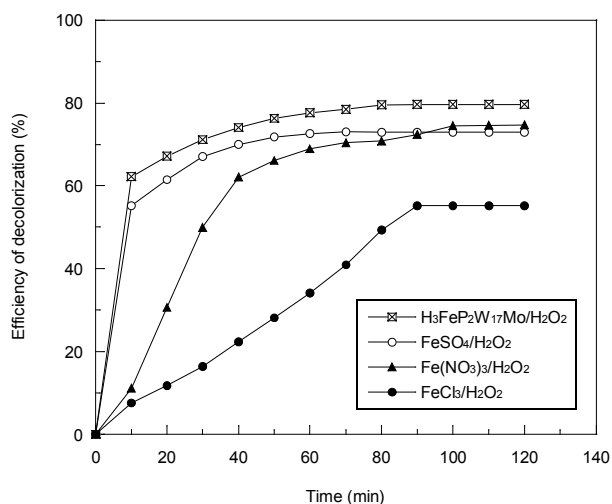


Fig. 14. Effect of the catalyst nature on the degradation of malachite green during Fenton oxidation catalysed by $\alpha_2\text{H}_3\text{FeP}_2\text{W}_{17}\text{MoO}_{62}$, FeSO_4 , $\text{Fe}(\text{NO}_3)_3$, FeCl_3 (Conditions: $V_R = 100$ mL, $[\text{MG}]_0 = 5$ mg/L; pH = 3, $[\text{Cat}] = 0.1$ mol/L, $[\text{H}_2\text{O}_2] = 0.31$ M, $T = 30^\circ\text{C}$).

located at 2,964.39 and 2,985.60 cm^{-1} are attributed to C-H bonds of CH_3 -group. The C = C bonds of the aromatic rings are present in the spectrum by their bands of low intensity located at 1,560 and 1,600 cm^{-1} . The OH group of the carboxylic acid was present in the bands at 2,600 and 2,700 cm^{-1} .

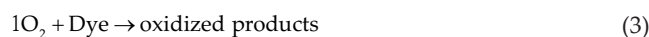
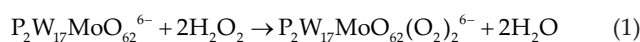
After 6 h of oxidation reaction, the IR spectrum showed no bands related to aromatic rings, and there were only bands of very low intensity relating to C-O and C = O groups of the carboxylic acid and a band located at 2,918.10 cm^{-1} was characteristic to C-H asymmetric vibration in alkyl group. Oxidation of MG was complete after 7 h of reaction where the IR spectrum in dichloromethane presented only bands thereof.

At the end of this study, we have compared the catalytic performance of the iron-substituted $\alpha_2\text{H}_3\text{FeP}_2\text{W}_{17}\text{MoO}_{62}$ (HPAFe) catalyst with three different iron catalysts used in Fenton process (FeSO_4 , FeCl_3 , $\text{Fe}(\text{NO}_3)_3$). The results are shown in following Fig. 14.

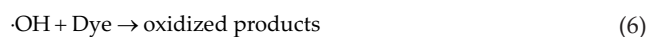
The results showed that, the efficiency of catalytic degradation varied significantly with the nature of the catalyst. The yields obtained with different catalysts are ($E_{\text{HPAFe}} = 82.32\%$; $E_{\text{FeSO}_4} = 72.94\%$; $E_{\text{FeCl}_3} = 55.16\%$; $E_{\text{Fe}(\text{NO}_3)_3} = 72.36\%$). The degradation of malachite green by hydrogen peroxide in the presence of heteropolyanion Dawson HPAFe was better than the other catalysts.

3.4. Catalytic mechanism of $\text{H}_3\text{FeP}_2\text{W}_{17}\text{MoO}_{62}$

It was reported that the presence of H_2O_2 with molybdates MoO_4^{2-} [35] or heteropolyanions [36] lead to the formation of molybdenum (Mo) peroxy complex, $\text{MoO}_2(\text{O}_2)_2^{2-}$ or peroxy-HPA, which are a strong oxidants and can oxidize the organic compounds by the direct oxygen transfer or by the singlet oxygen ($^1\text{O}_2$) generated from the peroxy-complex:



On the other hand, the $\text{Fe}^{3+}/\text{H}_2\text{O}_2$ system suggest the reduction of Fe^{3+} to Fe^{2+} . The formed Fe^{2+} then reacts with H_2O_2 to generate $\cdot\text{OH}$ radicals which are ready to degrade the organic compounds:



4. Conclusions

This study mainly reports the synthesis and spectroscopic characterization of a Dawson heteropolyanion $\alpha_2\text{H}_3\text{FeP}_2\text{W}_{17}\text{MoO}_{62}$ and its use in one of the advanced oxidation process, process Fenton ($\text{H}_2\text{O}_2/\text{HPA}$) for degrading a pollutant, green malachite.

The degradation study of the dye was performed with the optimization of some reaction parameters; initial pH of solution, mass of catalyst, concentration of the oxidant, temperature and dye concentration in order to achieve demineralization. The catalytic activity results showed that the optimum conditions for the maximum catalytic.

Degradation of malachite green was obtained at initial solution pH of 3, a catalyst mass of 0.03 g, an initial hydrogen peroxide concentration of 0.31 mol/L, at temperature of 30°C and initial malachite green concentration of 20 mg/L. UV-Vis spectra showed the disappearance of C = C and C = N bonds after 80 min and IR spectra showed the destruction of aromatics rings after 6 h of reaction and the demineralization of dye was achieved after 7 h.

References

- [1] F. Sayilkan, M. Asiltürk, P. Tatar, N. Kiraz, E. Arpaç, H. Sayilkan, Preparation of re-usable photocatalytic filter for degradation of Malachite Green dye under UV and vis-irradiation, J. Hazard. Mater., 148 (2007) 735–744.
- [2] M.A. Behnajady, B. Vahid, N. Modirshahla, M. Shokri, Evaluation of electrical energy per order (E_{EO}) with kinetic modelling on the removal of Malachite Green by US/UV/ H_2O_2 process, Desalination, 249 (2009) 99–103.
- [3] C.H. Chen, C.F. Chang, S.M. Liu, Partial degradation mechanisms of malachite green and methyl violet B by *Shewanella* decolorationis NT0U1 under anaerobic conditions, J. Hazard. Mater., 177 (2010) 281–289.

- [4] X.J. Zhou, W.Q. Guo, S.S. Yang, H.S. Zheng, N.Q. Ren, Ultrasonic-assisted ozone oxidation process of triphenylmethane dye degradation: evidence for the promotion effects ultrasonic on malachite green decolorization and degradation mechanism, *Bioresour. Technol.*, 128 (2013) 827–830.
- [5] S. Gokulakrishnan, P. Parakh, H. Prakash, Degradation of Malachite green by Potassium persulphate, its enhancement by 1,8-dimethyl-1,3,6,8,10,13-hexaazacyclotetradecane nickel (II) perchlorate complex, and removal of antibacterial activity, *J. Hazard. Mater.*, 213–214 (2012) 19–27.
- [6] Y.C. Lee, E.J. Kim, J.W. Yang, H.J. Shin, Removal of malachite green by adsorption and precipitation using aminopropyl functionalized magnesium phyllosilicate, *Desalination*, 192 (2011) 62–70.
- [7] F. Ding, X.N. Li, J.X. Diao, Y. Sun, L. Zhang, L. Ma, X.L. Yang, L. Zhang, Y. Sun, Potential toxicity and affinity of triphenylmethanedye malachite green to lysozyme, *Ecotoxicol. Environ. Safety*, 78 (2012) 41–49.
- [8] N. Bilandzic, I. Varenina, B.S. Kolanovic, D. Oraic, S. Zrncic, Malachite green residues in farmed fish in Croatia, *J. Food Contr.*, 26 (2012) 393–396.
- [9] J.F. Benitez, J. Beltran-Henadian, J.L. Acero, F.J. Rubio, Contribution of free radicals to chlorophenols decomposition by several advanced oxidation process, *Chemosphere*, 41 (2000) 1271–1277.
- [10] P. Bautista, A.F. Mohedano, M.A. Gilarranz, J.A. Casas, J.J. Rodriguez, Application of Fenton oxidation to cosmetic wastewaters treatment, *J. Hazard. Mater.*, 143 (2007) 128–134.
- [11] X. Fan, H. Hao, Y. Wang, F. Chen, J. Zhang, Fenton-like degradation of nalidixic acid with $\text{Fe}^{3+}/\text{H}_2\text{O}_2$: reactions, *Environ. Sci. Pollut. Res.*, 6 (2013) 3649–3656.
- [12] E. Neyens, J. Baeyens, A review of classic Fenton's peroxidation as an advanced oxidation technique, *J. Hazard. Mater.*, 1–3 (2003) 33–50.
- [13] J.K. Kim, J.H. Choi, J.H. Song, J. Yi, I.K. Song, Etherification of n-butanol to di-n-butyl ether over $\text{HnXW}_{12}\text{O}_{40}$ ($\text{X}=\text{Co}^{2+}$, B^{3+} , Si^{4+} , and P^{5+}) Keggin heteropolyacid catalysts, *Catal. Commun.*, 27 (2012) 5–8.
- [14] R. Gao, H. Chen, Le Yingyi, W.-L. Dai, K. Fan, Highly active and selective $\text{Cs}_{2.5}\text{H}_{0.5}\text{PW}_{12}\text{O}_{40}/\text{SBA-15}$ composite material in the oxidation of cyclopentane-1,2-diol to glutaric acid by aqueous H_2O_2 , *Appl. Catal. A*, 352 (2009) 61–65.
- [15] J. Wang, C. Hu, M. Jian, J. Zhang, G. Li, Catalytic oxidation performance of the α -Keggin-type vanadium-substituted heteropolymolybdates: a density functional theory study on $[\text{PVnMo}_{12-n}\text{O}_{40}]^{(3+n)-}$ ($n=0-3$), *Catalysis*, 240 (2006) 23–30.
- [16] M. Ammam, I.-M. Mbomekalle, B. Keita, L. Nadjo, J. Fransaer $[\text{As}_8\text{W}_{48}\text{O}_{184}]^{40-}$, a new crown-shaped heteropolyanion: electrochemistry and electrocatalytic properties towards reduction of nitrite, *Electrochim. Acta*, 55 (2010) 3118–3122.
- [17] B. Keita, E. Abdeljalil, L. Nadjo, R. Contant, R. Belghiche, Cooperativity of copper and molybdenum centers in polyoxometalate-based electrocatalysts: cyclic voltammetry, EQCM, and AFM characterization, *Langmuir*, 22 (2006) 10416–10425.
- [18] R. Belghiche, O. Bechiri, M. Abbessi, S. Golhen, Y. Le Gal, L. Ouahab, 2D and 3D polymeric Wells-Dawson polyoxometalates: synthesis, crystal structures, and cyclic voltammetry of $[(\text{M}(\text{H}_2\text{O})_4)_x][\text{H}_{6-2x}\text{P}_2\text{W}_{18-n}\text{MoO}_{62}]$ ($\text{M}=\text{Cu}^{\text{II}}$, Co^{II} , Ni^{II}), *Inorg. Chem.*, 48 (2009) 6026–6033.
- [19] F.F. Bamoharram, S.H. Niknezhad, J. Baharara, A. Ayati, M. Ebrahimi, M.M. Heravi, Amine-functionalized nanosilica-supported Dawson heteropolyacid: an eco-friendly and reusable photocatalyst for photodegradation of malachite green, *J. Nanostruct. Chem.*, 4 (2014) 88.
- [20] R. Massart, R. Contant, J.M. Fruchart, J.P. Ciabrini, M. Fournier, ^{31}P NMR studies on molybdc and tungstic heteropolyanions. correlation between structure and chemical shift, *Inorg. Chem.*, 16 (1977) 2916–2921.
- [21] R. Contant, J.P. Ciabrini, Préparation et propriétés des solutions de quelques hétéropolyanions lacunaires dérivés des 18-tungsto-2-phosphates (isomères α et β), *J. Chem. Res.*, (1977) 2601–2609.
- [22] B.H. Hameed, T.W. Lee, Degradation of malachite green in aqueous solution by Fenton process, *J. Hazard. Mater.*, 164 (2009) 468–472.
- [23] R. Contant, J.P. Ciabrini, Préparation et propriétés des solutions de quelques hétéropolyanions lacunaires dérivés des 18-tungsto-2-phosphates (isomères α et β), *J. Chem. Res.*, (1979) 2610–2618.
- [24] L. Li, M. Pengtao, W. Jingping, N. Jingyang, A new inorganic 2D network polyoxometalate constructed from Wells–Dawson phosphomolybdate linked through Cu (II) ions, *Inorg. Chem. Commun.*, 34 (2013) 23–26.
- [25] T. Yan, L. Li, G. Li, Y. Wang, W. Hu, X. Guan, Porous SnIn_4S_8 microspheres dyes degradation under visible light irradiation, *J. Hazard. Mater.*, 186 (2011) 272–279.
- [26] C. Rocchiccioli–Deltcheff, R. Thouvenot, Vibrational studies of heteropolyanions related to $\alpha\text{-P}_2\text{W}_{18}\text{O}_{62}^{6-}$, *Spectrosc. Lett.*, 12 (1979) 127–138.
- [27] C. Rocchiccioli – Deltcheff, R. Thouvenot, R. Franck, Spectres i.r. et Raman d'hétéropolyanions $\alpha\text{-XM}_{12}\text{O}_{40}^{n-}$ de structure de type Keggin ($\text{X}=\text{B}^{\text{III}}$, Si^{IV} , Ge^{IV} , P^{V} , As^{V} et $\text{M}=\text{W}^{\text{VI}}$ et Mo^{VI}), *Spectrochim. Acta Part A*, 32 (1976) 587–597.
- [28] R. Contant, M. Abbessi, J. Canny, M. Richet, B. Keita, A. Belhouari, L. Nadjo, Synthesis, characterization and electrochemistry of complexes derived from $[(1),2,3\text{-P}_2\text{Mo}_2\text{W}_{15}\text{O}_{61}]^{10-}$ and first transition metal ions, *Eur. J. Inorg. Chem.*, (2000) 567–574.
- [29] R. Belghiche, R. Contant, Y. Wei Lu, B. Keita, M. Abbessi, L. Nadjo, J. Mahuteau, Synthesis and characterization of Fe- or Cu-substituted molybdenum enriched tungstodiphosphates, *Eur. J. Inorg. Chem.*, (2002) 1410–1414.
- [30] L. Szpyrkowicz, C. Juzzolino, S.N. Kaul, A comparative study on oxidation of disperse dyes by electrochemical process, ozone, hypochlorite and Fenton reagent, *Water Res.*, 35 (2001) 2129–2136.
- [31] N.M. Mahmoodi, M. Arami, N.Y. Limaee, Photocatalytic degradation of triazinic ring containing azo dye (Reactive Red 198) by using immobilized TiO_2 photoreactor: bench scale study, *J. Hazard. Mater.*, 133 (2006) 113–118.
- [32] C. Bai, W. Xiao, D. Feng, M. Xian, D. Guo, Z. Ge, Y. Zhou, Efficient decolorization of Malachite green in the Fenton reaction catalyzed by $[\text{Fe}(\text{III})\text{-salen}]\text{Cl}$ complex, *Chem. Eng. J.*, 215–216 (2013) 227–234.
- [33] D.H. Williams, I. Fleming, *Spectroscopic Methods in Organic Chemistry*, 4th edn., McGraw-Hill, London 2006.
- [34] S. Kumar, G. Nanak, *Organic Chemistry, Spectroscopy of Organic Compounds*, Available online at: http://www.uobabylon.edu.iq/eprints/publication_11_8282_250.pdf, 2006, (Accessed on 05 June, 2014).
- [35] S.H. Tiana, Y.T. Tu, D.S. Chen, X. Chen, Y. Xiong, Degradation of acid Orange II at neutral pH using $\text{Fe}_2(\text{MoO}_4)_3$ as a heterogeneous Fenton-like catalyst, *J. Chem. Eng.*, 169 (2011) 31–37.
- [36] M. Moudjahed, L. Dermeche, S. Benadji, T. Mazari, C. Rabia, Dawson-type polyoxometalates as green catalysts for adipic acid synthesis, *J. Mol. Catal. A*, 414 (2016) 72–77.